

Received September 23, 2019, accepted October 14, 2019, date of publication October 21, 2019, date of current version November 1, 2019.

Digital Object Identifier 10.1109/ACCESS.2019.2948610

Research and Design of a Transmission System for Time-Frequency-Domain Electromagnetic Method

GANG LI , (Member, IEEE), **NAIJIA LIU, CHUNFENG ZHANG, AND CHANGSHENG LIU**

College of Instrumentation and Electrical Engineering, Jilin University, Changchun 130061, China

Corresponding author: Changsheng Liu (liuchangsheng@jlu.edu.cn)

This work was supported by the National Natural Science Foundation of China under Grant 51507073.


ABSTRACT In electromagnetic sounding, the detection areas of time-domain and frequency-domain electromagnetic detection methods cannot be effectively connected, and the detection processes for these two methods must be implemented separately. To combine time-domain and frequency-domain electromagnetic detection methods and simplify the detection process, a time-frequency fusion transmission method is proposed to simultaneously excite the earth to produce transient and steady-state responses. By analyzing the characteristics of the time-domain and frequency-domain excitation current waveforms, a pseudorandom transmission waveform with dead time is designed, and a transmission system for a time-frequency fusion electromagnetic detection method is developed. In this detection mode, the pseudorandom transmission waveform contains several frequencies, and the transient induction field can be received during the dead time. The time-domain and frequency-domain responses can be obtained by the same procedure. At the same time, a self-adaptive pseudoload device is designed and matched with the corresponding control sequence to reduce the influence of dead-time. The experimental results show that the self-adaptive pseudoload transmitter can effectively reduce the current fluctuation, and the time-frequency electromagnetic transmission system can effectively excite the earth to produce transient and steady-state responses. The time-frequency fusion electromagnetic transmission method proposed in this paper can be used in electromagnetic detection instruments to improve the efficiency of electromagnetic sounding.

INDEX TERMS Time-frequency fusion, electromagnetic transmission, turn-off dead time, self-adaptation pseudoload.

I. INTRODUCTION

Artificial field source electromagnetic detection plays an important role in mineral resource exploration, oil and gas resource exploration, geothermal resource development, geological engineering surveys, high-level radioactive waste disposal and other fields [1]–[6]. According to the different transmission waveforms and detection methods, the electromagnetic detection methods employed for artificial field sources are mainly divided into time-domain and frequency-domain electromagnetic detection methods. Time-domain electromagnetic detection method usually transmits a bipolar square wave current signal with a duty cycle of 50%. By detecting the secondary induced field, the spatial

distribution of the underground resistivity can be acquired [7], [8]. Because the secondary field signal in this method is weak for a long offset, it is usually detected in the near-source area. For a conventional grounded long wire source, the distance between the transmitter and receiver for the time-domain method is generally less than 3 km. The frequency-domain method transmits a continuous current waveform and obtains the resistivity distribution of different depths underground by collecting the amplitude and phase information of the electromagnetic field at different frequencies [9], [10]. Because the frequency-domain method collects steady-state signals, it can achieve detection over a wide range. However, this method is mainly applicable to the far region [11]. The receiving and transmitting distances are generally more than 3-5 times the skin depth, usually greater than 6 km [12]. Therefore, both the time-domain and

The associate editor coordinating the review of this manuscript and approving it for publication was M. A. Hannan .

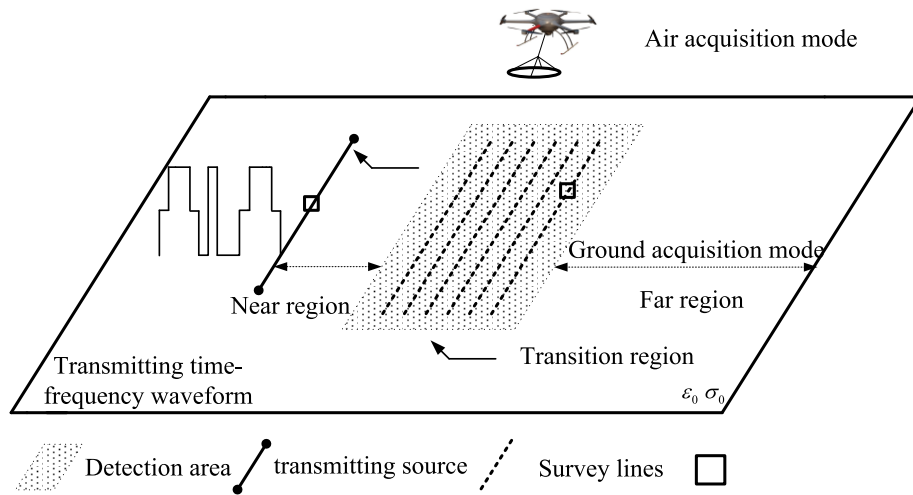


FIGURE 1. Diagram of the time-frequency electromagnetic detection system.

frequency-domain methods have their own applicable ranges. The detection areas of the two methods cannot be effectively connected. There is a detection blind area, and the whole detection area cannot be achieved by using a single transmitter. In addition, due to the different transmission waveforms, conventional time-domain and frequency-domain methods cannot be employed simultaneously.

In practical detection, when the environmental noise is large, especially for the latest development in semi-airborne electromagnetic detection methods [13], [14], the detection distance between the transmitter and receiver is mainly concentrated in the range of 0.5-6 km. In this case, the nonplanar wave region near the transmitter is transformed into the core detection area. Conventional detection methods and transmission waveforms cannot cover the whole area effectively. To expand the detection range, He Ji-shan proposed a wide-area electromagnetic detection method [15] that extended the frequency-domain detection range from the far region to the transition region. Due to the influence of stratum waves in the near-source area, the method has a limited extension range and cannot achieve a seamless connection between the time-domain and frequency-domain detection areas. Zhan-Xiang *et al.* proposed a time-frequency electromagnetic detection method for oil and gas target detection and evaluation [16]–[18]. The method can collect signals in the time domain and frequency domain at the same time, extract resistivity and polarizability information according to the two signals, and complete a prediction of the oil and gas targets. In the early stage, the method only transmits the current waveform in the frequency domain, including the field source effect and primary field noise. In the later stage, the frequency-domain current waveform and time-domain current waveform are transmitted independently. By eliminating the effect of field source effects and the primary field through the time-domain waveform, the detection area is expanded and can be detected in the transition area. However,

because the method is based on the conventional transmission waveform and detection method, it must transmit the waveform in the time-domain and frequency-domain separately for acquisition, the detection efficiency is low and the expansion area is limited.

To realize a seamless connection between the detection areas in the time-domain and frequency-domain, improve the detection efficiency and focus on detection in transition areas covered by nonplanar waves, a time-frequency fusion electromagnetic transmission method is proposed, and a new pseudorandom time-frequency fusion transmission waveform is designed. Based on the transmission waveform, the time-frequency fusion transmitter and control system are studied. To solve the problem associated with the output current fluctuation caused by the turn-off dead time in the time-frequency waveform, a self-adaptive pseudoload device and control method are designed. The transmission system with the self-adaptive pseudoload device designed in this paper can effectively suppress the fluctuation of the transmission current. The proposed transmission waveform and transmission method can excite both the transient response in the time-domain and the steady-state response in the frequency-domain, improve the detection efficiency, and provide a new method to further develop the area of electromagnetic detection in general.

II. TIME-FREQUENCY FUSION ELECTROMAGNETIC TRANSMISSION METHOD

The diagram of time-frequency fusion electromagnetic detection is shown in Fig. 1. To improve the detection efficiency and adapt to the complex terrain structure, the actual detection strategy mainly lays a long grounding wire to supply current to the ground and uses the receiving system on an unmanned aerial vehicle (UAV) to collect the magnetic field in the sky. Because the acquisition time is short and the motion noise in UAV increases, the signal-to-noise ratio (SNR) of the data

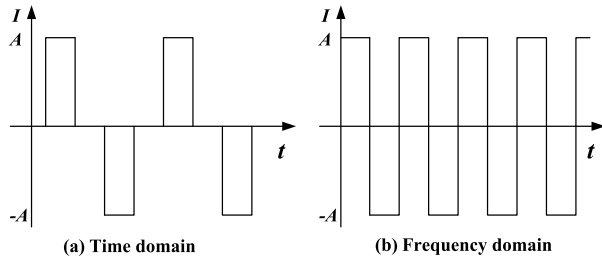


FIGURE 2. Typical time-domain and frequency-domain transmission waveforms.

decreases, so the transition region of the nonplanar wave incidence becomes the core detection area. To overcome the field source effects of the frequency-domain method and complete whole-area detection from the near source to the far source, it is necessary to correct the far-source frequency-domain interpretation through a near-source time-domain interpretation and reveal the complete underground resistivity structure by combining the two methods. In terms of detection, the time-domain transient response and the frequency-domain steady-state response should be collected simultaneously in one detection process for time-frequency fusion electromagnetic detection.

A. CONVENTIONAL TRANSMISSION CURRENT WAVEFORM

In conventional detection, the transient response and steady-state response are obtained by an independent time-domain excitation and frequency-domain excitation, respectively. Typical transmission waveforms in the time-domain and frequency-domain are shown in Fig. 2.

Time-domain methods usually detect the secondary field response after the earth is stimulated. To eliminate the influence of the transmission source on the measured signal, it is necessary to add a 0-level excitation to the transmission waveform. The typical time-domain current waveform is a bipolar square wave with a duty cycle of 1:1. The transition process of the secondary field during the turn-off time can be divided into two stages: the early signal mainly reflects the shallow information, and the late signal mainly reflects the deep information. In a uniform half-space, the diffusion depth in the time domain is determined by equation (1) [19]:

$$h = \sqrt{\frac{2tp}{\mu}} \quad (1)$$

In the formula, h represents the detection depth, t represents the duration of the zero level in the transmission waveform, μ represents the permeability of the medium, and ρ represents the uniform earth electrical resistivity. To achieve large-depth detection, the duration of the 0 level is usually increased.

Typical transmission waveforms of the frequency-domain electromagnetic detection method are shown in Fig. 2 (b). The transmission waveforms are excited by a square wave

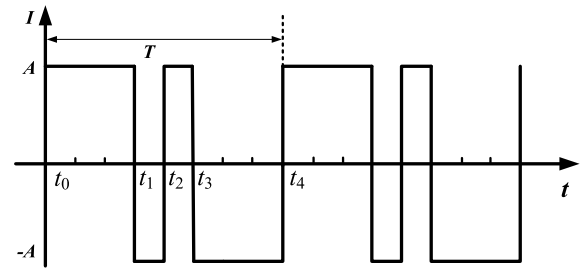


FIGURE 3. Pseudorandom transmission waveform.

and do not contain a zero-level switch-off. In this method, the frequency of the electromagnetic field is changed to achieve sounding. In the uniform half-space, the skin depth is usually determined by formula (2):

$$\delta = 503 \sqrt{\frac{\rho}{f}} \quad (2)$$

In the formula, δ represents the depth of detection, and f represents the frequency of the transmission current. For a square wave, due to the attenuation of the harmonic signal, the fundamental frequency is used for each transmission. Formula (2) shows that one transmission frequency corresponds to one detection depth. If the ground resistivity information of different depths must be detected, square wave signals of different frequencies must be transmitted accordingly. The number of experiments increases, and the detection efficiency decreases. To improve the detection efficiency, He Ji-shan proposed a $2n$ sequence pseudorandom transmission current waveform [20] for frequency-domain detection. The waveform increases the available spectrum of the signal by changing the zero-crossing frequencies and the zero-crossing time of the adjustment signal. Figure 3 shows the three-frequency pseudorandom transmission waveform. There are four waveform flips (t_1 , t_2 , t_3 , and t_4) in one cycle T . In the first half cycle (t_0 - t_2), the ratio of the high to low level duration is 3:1. The latter half cycle waveform and the former half cycle waveform form a centrosymmetric odd function. Fig. 4 shows the signal spectrum of the fundamental frequency (12 Hz) square wave and the three-frequency pseudorandom wave. The simulation results show that the square wave spectrum contains only odd harmonics, and the amplitude of each harmonic decreases rapidly with an increase in frequency. The spectrum of the three-frequency pseudorandom wave contains many frequency harmonics, in which the amplitudes of the fundamental, second and fourth harmonics are larger and approximately equal. It can be seen that the pseudorandom waveform is helpful for improving the detection efficiency compared with the single-frequency square wave transmission mode.

B. DESIGN OF THE TIME-FREQUENCY FUSION TRANSMISSION CURRENT WAVEFORM

Based on the multifrequency characteristics of the pseudorandom signal, a 2^n sequence pseudorandom signal is used

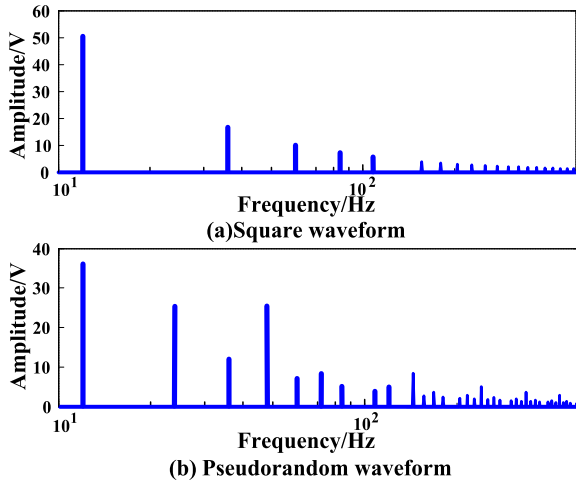


FIGURE 4. Comparison of the spectra of the square waveform and pseudorandom waveform.

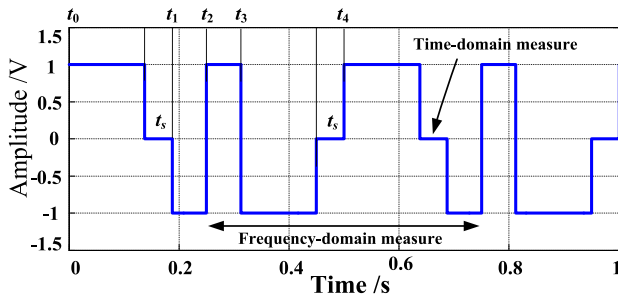


FIGURE 5. Time-frequency emission current waveform.

to design the time-frequency fusion transmission waveform such that it meets the requirements for time-frequency detection and the acquisition of the time-domain transient response and frequency-domain steady-state response. To ensure the stability and controllability of the excitation frequency and harmonic frequency, the waveform period and the number of flips are kept unchanged in the fusion design. To achieve the maximum time-domain excitation response, a zero-level continuation process is introduced at the end of the high and low levels with the longest duration to ensure that one transient response is excited in both the positive and negative directions in one cycle. Fig. 5 shows a typical time-frequency fusion transmission waveform. The transmission waveform is based on a three-frequency pseudorandom wave. Within a period of T , the waveform changes t_1, t_2, t_3 and t_4 are consistent with the conventional pseudorandom wave. In the first high-level stage (t_0-t_1) with the longest duration and the corresponding low-level stage (t_3-t_4), the zero level is introduced as the turn-off dead time to excite the transient response in the time domain. The zero-level duration is t_s , which is determined by the depth of the target. In practical detection, the steady-state response in the frequency domain can be obtained by detecting the signal in the whole period, and the transient response in the time domain can be obtained by detecting the signal in the turn-off dead time. The two responses in

the detection area can be obtained simultaneously through the transmission current waveform.

According to the design principle of the time-frequency fusion current waveform, by satisfying the detection of the transient response in the time domain and steady-state response in the frequency domain, the expression of the new pseudorandom time-frequency fusion waveform can be expressed as follows:

$$p(2, n, t) = \begin{cases} A & 0 \leq t < \frac{l_1 T - t_s}{2^n} \\ 0 & \frac{l_1 T - t_s}{2^n} \leq t < \frac{l_1 T}{2^n} \\ -A & \frac{l_1 T}{2^n} \leq t < \frac{l_2 T}{2^n} \\ \dots & \dots \\ -A & \frac{l_{m-1} T}{2^n} \leq t < \frac{l_m T - t_s}{2^n} \\ 0 & \frac{l_m T - t_s}{2^n} \leq t < \frac{l_m T}{2^n} = T \end{cases} \quad (3)$$

In the formula, A is the amplitude, $l_k (k = 1, 2, \dots, m)$ are integers, m represents the number of the polarity changes, and t_s is the dead time, which changes according to the detection depth of the transient response in the time domain. According to the time-series expression of the pseudorandom time-frequency fusion waveform, the signal amplitude of the target frequency point can be obtained by a Fourier transform, and the influence of the dead time on the signal amplitude can be analyzed. For the convenience of analysis, the amplitude of the time-frequency fusion waveform is set to 1. For a transmission current waveform with a period of T , the k -th harmonic amplitude expression is [21]:

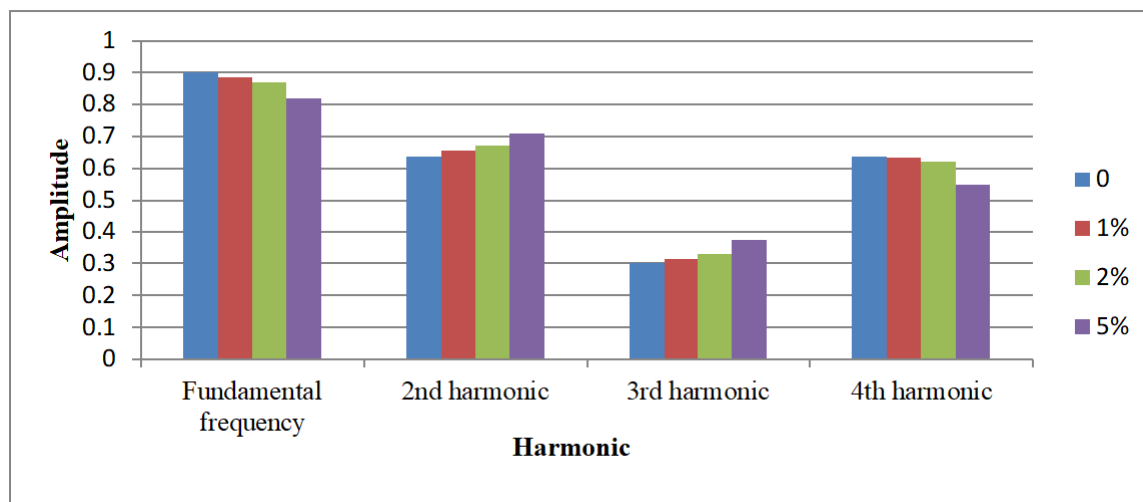
$$A_{km} = \left| \frac{2}{k\pi} \sum_{m=1}^M (-1)^{m-1} e^{j\omega_k \tau_m} \sin \left[\omega_k \left(\Delta t_m - \frac{t_s}{2} \right) \right] \right|$$

$$\omega_k = k\omega, \quad \tau_m = \frac{1}{2}(t_m + t_{m-1}), \quad \Delta t_m = \frac{1}{2}(t_m - t_{m-1}) \quad (4)$$

ω_k in the formula represents the harmonics of the transmission current waveform and t_m represents the time length of the positive and negative polarity of the current. A three-frequency pseudorandom time-frequency wave with a transmission frequency of 1 Hz is selected for the study. Table 1 shows the spectrum amplitude of each frequency point of the transmitted waveform current at different dead times. When $t_s = 0$ s, the time-frequency fusion waveform is transformed into the conventional three-frequency pseudorandom waveform. From Fig. 6, it can be found that with an increase in the dead time, the amplitudes of the fundamental wave and fourth harmonic decrease, and the amplitudes of the second and third harmonic increase. When the dead time reaches 0.05 s, that is, the ratio of the dead time is 5%, the components of each main frequency are similar to those with zero dead time, and the designed time-frequency fusion transmission current waveform can still meet the detection requirements of multiple frequency points and high efficiency in the frequency domain. At the same time, the introduction

TABLE 1. Effect of DEAD-TIME on spectrum.

Duty cycle of dead-time	Fundamental frequency	2th harmonic	3th harmonic	4th harmonic
0	0.9003	0.6366	0.3001	0.6366
1%	0.8858	0.6557	0.3147	0.6329
2%	0.8704	0.6727	0.33	0.6217
5%	0.8193	0.7107	0.3737	0.548

**FIGURE 6.** Effect of dead-time on the spectrum.

of a long dead time can also meet the detection requirements of a large depth in the time domain. In practical applications, the frequency of the time-frequency fusion waveform and dead time can be set according to the depth of the target body such that the transient response and steady-state response can be obtained.

III. DESIGN OF THE TIME-FREQUENCY TRANSMISSION SYSTEM

The electromagnetic transmission system is powered by a generator or battery. Based on power semiconductor devices and the corresponding circuit topology, it can output a specific current waveform through converter technology and excite an alternating electromagnetic field in space. A time-domain transmission system is usually loaded with an ungrounded coil. Due to the low resistance and high inductance of the load coil, the power of a time-domain transmission system is generally low, and the response time of the natural current turn-off process is long. It is necessary to design a specific circuit structure to reduce the turn-off time [22]. A frequency-domain transmission system usually employs long grounded wires to excite the electromagnetic field, and the load has a high resistance and low inductance [23]. Compared with the turn-off time for a time-domain transmission system, the natural turn-off time of the current waveform in a frequency-domain transmission

system is shorter and the transmitting power is higher. For conventional detection, the transmission power is usually tens of kilowatts; for deep detection, the power of the transmission system can reach hundreds of kilowatts. To achieve large-scale and deep detection, a time-frequency transmission system is designed based on a frequency-domain grounding load transmission system.

For conventional frequency-domain waveforms, the output power of the transmission system is constant in one cycle. In the time-frequency fusion transmission mode, there is an abrupt power change in the transmission system due to the introduction of dead time. In the dead time, the output current of the transmitter is 0 A, and the generator is in a no-load state; in the high- and low-level stages, the output current of the transmitter is $\pm A$, and the generator is in the full-load state. For a high-power transmission system, when the generator is switched between the full-load and no-load states frequently, the generator life will be reduced and the stability will decline. In addition, due to the limitation of the self-regulation accuracy and response time of the DC power supply and current-stabilized circuit, the abrupt change in the transient power will also lead to distortion in the output current waveform, which will affect the detection accuracy. To eliminate the impact of an abrupt power change, a time-frequency transmission system with a self-adaptive pseudoload is designed in this paper. During the dead time of

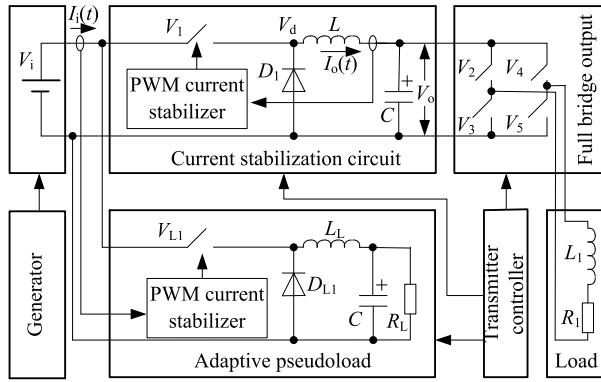


FIGURE 7. Schematic diagram of the transmission system.

the transmission current, the power release loop is employed with a self-adaptive pseudoload to restrain the abrupt change in the power and avoid a fluctuation in the transmission current.

Fig. 7 shows a schematic diagram of the time-frequency transmission system. It includes a generator, DC power supply, current stabilization circuit, full-bridge output, self-adaptive pseudoload and transmitter controller. The generator outputs a three-phase alternating current to provide electrical energy to the whole system. The DC power supply regulates the three-phase AC, outputs a stable voltage V_i , and provides DC power to the current-stabilizing circuit and self-adaptive pseudoload. The current stabilization circuit uses a pulse width modulation (PWM) algorithm to control the output current such that it is constant [24]. The current is inverted by the full-bridge circuit to output the preset excitation waveform to the earth load. The self-adaptive pseudoload is connected in parallel with the current stabilizer circuit, which is powered by the DC power supply and controlled by the transmitter controller. The controller is the core of the whole system, which adjusts the working state and parameters of each circuit in the transmission system.

Fig. 8 shows the control sequence of the transmitter controller. A is the preset transmission waveform of the controller, and ENB is the overall enabling signal of the system. Its high-level indicates whether or not the current waveform is output to the earth. G_1 and G_2 are the driving signals of the inverted H-bridge switches V_3, V_4, V_2 and V_5 . High and low levels indicate the turn-on and turn-off states of the switches, respectively. Consider the definition:

$$G = (G_1 + G_2) \cdot ENB \quad (5)$$

Thus,

$$G_3 = ENB \cdot \bar{G} \quad (6)$$

In the formula, “+”, “.” and “-” represent “or”, “and” and “not” logic operations, respectively. G is the enabling control signal of the current-stabilizing circuit. Its high-level indicates the turn-on and turn-off states of the current-stabilizing circuit. G_3 is the enabling control signal of the self-

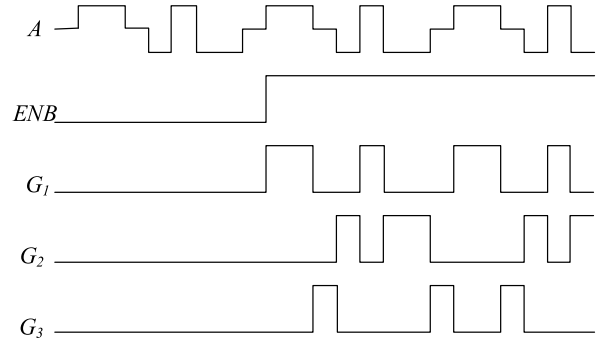


FIGURE 8. Emission control sequence.

adaptive pseudoload, and its height indicates the turn-on and turn-off states of the self-adaptive pseudoload circuit.

In the high-level stage of the preset waveform A , the driving signal G_1 has a high level, the switches V_3 and V_4 turn on, and the current flows forward to the ground load. In the low-level stage of the preset waveform A , the driving signal G_2 has a high level, the switches V_2 and V_5 turn on, and the current flows backwards to the ground load. In the high- and low-level stages of the preset waveform, the enabling control signal G has a high level, and the current stabilizing circuit operates normally. In the zero-level stage of the preset waveform A , the G_1 and G_2 signals are low and the G_3 signal is high. At this time, the current stabilizer circuit and the output bridge stop working, and the self-adaptive pseudoload works. The transmission power is matched by the resistive load R_L .

The self-adaptive pseudoload device uses a buck circuit topology and PWM algorithm to adjust the output current to achieve power matching. To ensure a constant output current of the DC power supply, the control circuit of the self-adaptive pseudoload reads the output current $I_i(t)$ of the power supply continuously when G_3 has a low level. When G_3 changes from a low level to a high level, the control circuit locks to the output current $I_i(t_f)$ of the power supply corresponding to t_f at the previous time. When G_3 has a high level, the power circuit of the self-adaptive pseudoload operates. The output voltage of the load is adjusted by the second PWM current stabilizer, so that the output current $I_i(t)$ of the power supply equals $I_i(t_f)$. To realize the adaptive function, the resistive load is matched according to the maximum transmitting power:

$$R_L = V_i^2 / P_{\max} \quad (7)$$

When the power of the output bridge changes, the second PWM current stabilizer automatically adjusts the output current for power matching. The stability of the output current on the bus can be guaranteed by the self-adaptive pseudoload circuit and response control logic, which can prevent the transient impact an abrupt power change on the transmitter and reduce the fluctuation of the output current of the grounding load.

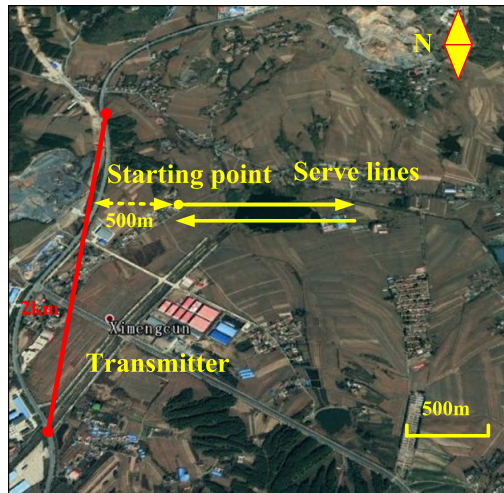


FIGURE 9. Layout map of field test lines.

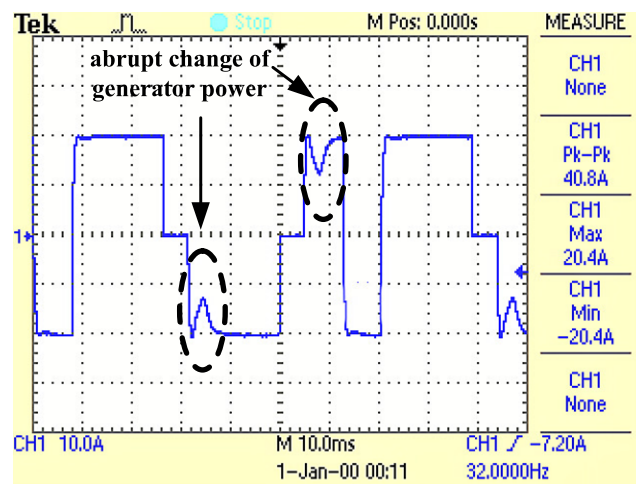


FIGURE 10. Current waveform without an adaptive load.

IV. EXPERIMENTAL TEST

To verify the stability and incentive effect of the designed transmitting system, a time-frequency transmitting test was carried out in the goaf of Liaoyuan Coal Mine, Jilin Province, in November 2017. The layout of field detection lines is shown in Fig. 9. The transmitting source is in the north-south direction and is laid along the highway. The length of the line is 2 km. The survey line is east-west, starting point is 500 meters away from the transmitting source, and the length of the survey line is 1 km. It is located in the transitional zone. During the test, the current station was used to record the current waveform transmitted, and the receiving system developed by the research group was used to record the induction voltage signal produced by the coil sensor.

A. THE ADAPTIVE PSEUDO LOAD TEST

Figs. 10 and 11 show the time-frequency current waveforms transmitted by different transmitters. The transmission waveform in Fig. 10 is for a conventional frequency-domain transmitter without a self-pseudoload. At the end of

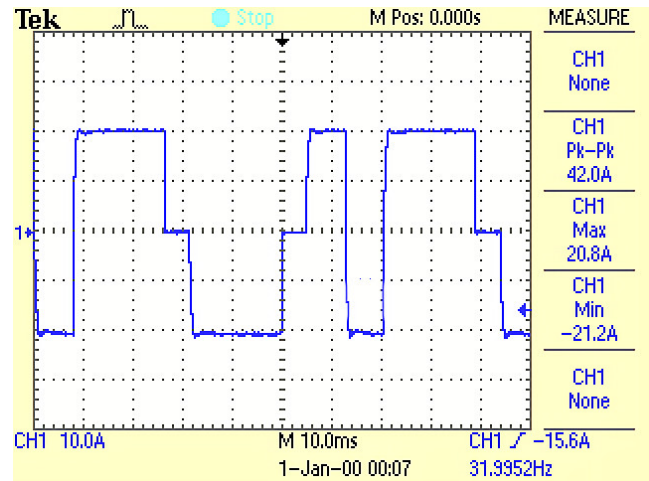


FIGURE 11. Current waveform with an adaptive load.

the dead time, when the current waveform changes to $\pm A$, the current waveform will be distorted. Due to the sudden power change and feedback lag of the generator and transmitter system, the current decreases rapidly after reaching the highest point, the maximum amplitude reduction is close to 8 A, and the distortion duration is approximately 8 ms. The waveform distortion will seriously affect the detection accuracy of the acquisition signal. Fig. 11 shows the current waveform generated by the time-frequency transmission system with the self-adaptive pseudoload designed in this paper. At high and low levels, the amplitude of the current waveform is constant. By comparing the results of the two tests, it can be concluded that in the time-frequency transmission mode, the self-adaptive pseudoload can effectively suppress the abrupt change in the generator power caused by the introduction of the turn-off dead time, the distortion in the transmission current waveform is obviously improved, and the current amplitude is stable.

B. TEST RESULTS OF THE RECEIVING SYSTEM

Using the time-frequency transmission system with the self-adaptive pseudoload, according to the requirements of the detection depth and resolution ratio, the base frequency of the transmission current is 16 Hz, the dead time is 5 ms, and the transmission current is 40 A. Fig. 12 (a) shows the acquisition signal, in which the red line shows the transmission current and the blue line shows the induced voltage signal. When the transmission current changes, the receiving system collects the transient induced voltage signal. The upward current change excites the positive transient attenuation signal, while the downward current change excites the negative transient attenuation signal. The amplitude of the attenuation signal is proportional to the change in the current. At times t_2 and t_3 , the amplitude of the transient response caused by the excitation is larger because of the large change in the current. Note that in the conduction phase of the transmission system, a change in the current and coil orientation will easily

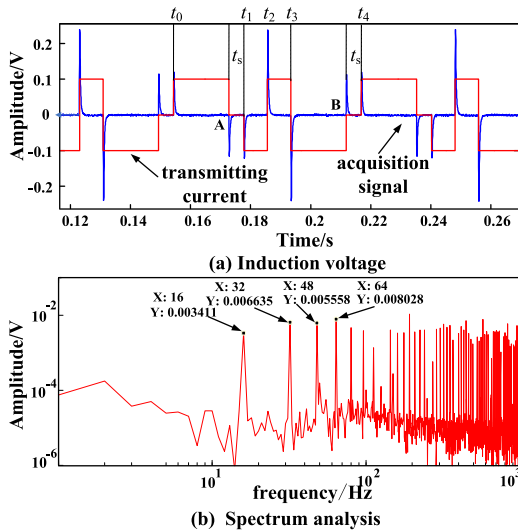


FIGURE 12. Analysis of the acquisition signal.

introduce primary field noise, resulting in a large detection error.

Therefore, the secondary field response is usually detected in the 0-level stage. The attenuation signal at position A and position B in the figure is an effective detection signal. Fig. 12 (b) shows the spectrum of the acquisition signal. At 16 Hz, 32 Hz, 48 Hz and 64 Hz, a strong induction voltage signal can be observed, which is much higher than the noise level and sufficient for the frequency-domain electromagnetic detection method. The above test results show that the designed time-frequency transmission method and system can excite the earth to produce a transient response and a steady-state response simultaneously. Time-domain detection and frequency-domain detection are realized simultaneously, which greatly improves the detection efficiency.

V. CONCLUSION

This paper proposes a time-frequency fusion transmission method for electromagnetic sounding to solve the problems associated with the blind areas in the ranges of time-domain and frequency-domain detection. The fusion transmission current contains two kinds of excitation waveforms, and the corresponding responses can be achieved simultaneously. The fusion transmission system is designed, and a self-adaptive pseudoload is used to suppress the abrupt change in the transmitting power and waveform distortion caused by dead time. Field experimental results show that the designed time-frequency transmission system with a self-adaptive pseudoload can effectively suppress the abrupt change in the generator power, eliminate the waveform distortion, and ensure the stability of the transmission current. In addition, the attenuation curve of the transient response caused by the dead time can be detected in the collected data, and the target frequency signal can be detected in the signal spectrum with a high signal-to-noise ratio, obtaining the transient response and steady-state response with a single detection process. The research content of this paper verifies the feasibility

of the time-frequency electromagnetic transmission method, improves the detection efficiency, expands the detection area, and lays a foundation for further study of time-frequency whole-area underground target detection.

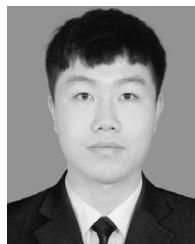
REFERENCES

- [1] S. N. Sheard, T. J. Ritchie, E. Brand, and K. R. Christopherson, "Mining, environmental, petroleum, and engineering industry applications of electromagnetic techniques in geophysics," *Surv. Geophys.*, vol. 26, no. 5, pp. 653–669, 2005.
- [2] M. E. Everett, "Theoretical developments in electromagnetic induction geophysics with selected applications in the near surface," *Surv. Geophys.*, vol. 33, no. 1, pp. 29–63, 2012.
- [3] G. Muñoz, "Exploring for geothermal resources with electromagnetic methods," *Surv. Geophys.*, vol. 35, no. 1, pp. 101–122, 2014.
- [4] R. Streich, "Controlled-source electromagnetic approaches for hydrocarbon exploration and monitoring on land," *Surv. Geophys.*, vol. 37, no. 1, pp. 47–80, 2016.
- [5] Q. Di, G. Xue, D. Lei, Z. Wang, Y. Zhang, S. Wang, and Q. M. Zhang, "Geophysical survey over molybdenum mines using the newly developed M-TEM system," *J. Appl. Geophys.*, vol. 158, pp. 65–70, Nov. 2018.
- [6] Z. An, Q. Di, C. Fu, C. Xu, and B. Cheng, "Geophysical evidence through a CSAMT survey of the deep geological structure at a potential radioactive waste site at Beishan, Gansu, China," *J. Environ. Eng. Geophys.*, vol. 18, no. 1, pp. 43–54, 2013.
- [7] C. C. Yin, B. Zhang, Y. H. Liu, X. Y. Ren, Y. F. Qi, Y. F. Pei, C. K. Qiu, X. Huang, W. Huang, J. J. Miao, and J. Cai, "Review on airborne EM technology and developments," (in Chinese), *Chin. J. Geophys.*, vol. 58, no. 8, pp. 2637–2653, 2015.
- [8] Y. Ji, Y. Zhu, M. Yu, D. Li, and S. Guan, "Calculation and application of full-wave airborne transient electromagnetic data in electromagnetic detection," *J. Central South Univ.*, vol. 26, no. 4, pp. 1011–1020, 2019.
- [9] X. He, H. Wang, and S. Ma, "Translation algorithm of the apparent conductivity using the frequency-domain electromagnetic method of a magnetic dipole," *J. Appl. Geophys.*, vol. 146, pp. 221–227, Nov. 2017.
- [10] J.-X. Liu, P.-M. Liu, and X.-Z. ong, "Three-dimensional land FD-CSEM forward modeling using edge finite-element method," *J. Central South Univ.*, vol. 25, no. 1, pp. 131–140, 2018.
- [11] D. Hou, G. Xue, N. Zhou, S. Yan, and Q. Di, "A new infinitesimal computational approach to calculating frequency-domain electromagnetic response," *J. Appl. Geophys.*, vol. 159, pp. 312–318, Dec. 2018.
- [12] W. Chen and G.-Q. Xue, "Effective skin depth of whole EM field due to a grounded wire source," (in Chinese), *Chin. J. Geophys.*, vol. 57, no. 7, pp. 2314–2320, 2014.
- [13] L. Kang, L. Liu, C. Liu, F. Zhou, and Z. Shi, "Forward modeling and analyzing for frequency domain semi-airborne EM method," in *Proc. Int. Workshop Gravity, Elect., Magn. Methods Appl.*, Chengdu, China, Apr. 2015, pp. 366–369.
- [14] H. Ito, H. Kaieda, T. Mogi, A. Jomori, and Y. Yuuki, "Grounded electrical-source airborne transient electromagnetics (GREATEM) survey of Aso Volcano, Japan," *Explor. Geophys.*, vol. 45, no. 1, pp. 43–48, 2014.
- [15] J.-S. He, "Wide field electromagnetic sounding method," (in Chinese), *J. Central South Univ., Sci. Technol.*, vol. 41, no. 3, pp. 1065–1072, 2010.
- [16] W. Zhi-Gang, H. Zhan-Xiang, and Q. Jing-Cheng, "New progress and application effect of time-frequency electromagnetic technology," (in Chinese), *Petroleumgeophys. Prospecting*, vol. 51, pp. 144–151, 2016.
- [17] Z. He, W. Hu, and W. Dong, "Petroleum Electromagnetic Prospecting Advances and Case Studies in China," *Surv. Geophys.*, vol. 31, no. 2, pp. 207–224, 2010.
- [18] H. Zhanxiang, S. Xiaodong, H. Zuzhi, S. Yanling, S. Dongyang, and D. Weibin, "Time-frequency electromagnetic method for exploring favorable deep igneous rock targets: A case study from north Xinjiang," *J. Environ. Eng. Geophys.*, vol. 24, no. 3, pp. 215–224, 2019.
- [19] B. R. Spies, "Depth of investigation in electromagnetic sounding methods," *Geophysics*, vol. 54, no. 7, pp. 872–888, 1989.
- [20] H. Ji-Shan, "Research of pseudo-random triple-frequencies electrical method," (in Chinese), *Chin. J. Nonferrous Metals*, vol. 4, no. 1, pp. 1–7, 1994.
- [21] R. Mittet and T. Schaug-Pettersen, "Shaping optimal transmitter waveforms for marine CSEM surveys," *Geophysics*, vol. 73, no. 3, pp. F97–F104, 2008.

[22] J. Lin, Y. Yang, X. Hu, and S. Wang, "Transmitting waveform control technology for transient electromagnetic method based on inductive load," (in Chinese), *J. Jilin Univ., Eng. Technol. Ed.*, vol. 46, no. 5, pp. 1718–1724, 2016.

[23] Z. Qi-Hui, Q.-Y. Di, and H.-B. Liu, "Key technology study on CSAMT transmitter with excitation control," (in Chinese), *Chin. J. Geophys.*, vol. 56, no. 11, pp. 3751–3760, 2013.

[24] K. Xue, F. Zhou, S. Wang, and J. Lin, "Constant-current control method of multi-function electromagnetic transmitter," *Rev. Sci. Instrum. Geophys. Prospecting*, vol. 86, no. 2, 2014, Art. no. 024501.



NAIJIA LIU received the bachelor's degree from Jilin University, in 2018. He is currently a graduate student with Jilin University, Changchun, China. His current research interests include high-power launcher and the data processing of semi-airborne electromagnetic detection systems.



CHUNFENG ZHANG received the bachelor's degree from Jilin University in 2018, where he is currently a graduate student. His current research interests include semi-airborne electromagnetic detection instrument and electromagnetic detection data processing.



GANG LI received the Ph.D. degree in electrical engineering from Tsinghua University, Beijing, China. He is currently an Associate Professor with the College of Instrumentation and Electrical Engineering, Jilin University, Changchun, China. His research interests include the modeling of semiconductors and Li-batteries, matrix converters, DC/DC power converter and its applications in electromagnetic detection instruments, and the design and implement of high power source.



CHANGSHENG LIU received the B.Sc. degree from Central South University, in 2003, and the Ph.D. degree from Jilin University, in 2009. He is currently a Professor and the Vice President of the College of Instrument and Electrical Engineering, Jilin University. His current research interest includes electromagnetic detection method and apparatus.

...